The Shapes of Neurotransmitters by Millimeter-Wave Spectroscopy: 2-Phenylethylamine

Peter D. Godfrey,* Lynette D. Hatherley, and Ronald D. Brown

Contribution from the Centre for High-Resolution Spectroscopy & Opto-electronic Technology, Chemistry Department, Monash University, Clayton, Victoria 3168, Australia

Received April 5, 1995[⊗]

Abstract: We have detected two conformers, (x) and (y), of 2-phenylethylamine and determined their shapes using microwave spectroscopy. By comparing observed and *ab initio* predicted spectroscopic rotational constants, dipole moments, amino-deuteration isotopic substitution coordinates, and the ^{14}N quadrupole coupling hyperfine patterns, species (x) has been identified with conformer **III** and species (y) with conformer **II** (see Figure 2). Both conformers are *gauche* with **III** being present in greater concentration. No other conformers occur in significant concentration in the vapor. Molecular orbital calculations correctly predict that **III** and **II** are the two most stable conformers. However at the RHF level the *ab initio* calculations predict that other conformers are of comparable stability to **II**, indicating that predictions of the relative energies of the conformers are not entirely reliable. When electron correlation is included at the MP2 level, the predicted energies of **III** and **II** are sufficiently lower than those of all the other conformers that their mole fractions in the prejet vapor at 120 °C would be too low for detection of the species in the jet spectrometer. A limited *ab initio* study of some of the barriers to conformer relaxation indicates that they are too high (>1000 cm^{-1}) for relaxation of the less stable conformers to **III** or **II**, except in the case of **I** where the low barrier to relaxation to **III** (about 270 cm^{-1}) implies that it would rapidly relax to **III** in the jet.

Introduction

2-Phenylethylamine (hereinafter abbreviated to phenylethylamine or PEA) is the simplest of a group of amine compounds which function in biological systems as neurotransmitters. It is most likely produced in the brain from the decarboxylation reaction of the α-amino acid, phenylalanine. The ethylamino side chain on a conjugated ring system is also present in other neurotransmitters such as amphetamine, serotonin, dopamine, histamine, and in related molecules such as noradrenaline.

The connection of phenylethylamine with human emotions and its identification as the "love drug" has been recently the subject of popular interest.[1a,b] The theory, apparently lying somewhere between popular myth and legitimate medical science, is that the euphoric feeling associated with falling in love is due to the increased production of phenylethylamine in the brain.

In support of the foregoing, the concentration of phenylethylamine in the human brain has been found to be highest in the limbic system,[2] where it is understood emotion and learning are controlled. It has been linked to paranoid chronic schizophrenia,[3] because people with this condition have been found to have higher than normal levels of phenylethylamine in the excreted urine. This was also the case in studies of people suffering profound stress.[4]

The issue as to whether the neutral or protonated form is pharmacologically active is not clear-cut. The answer appears to vary and lies in the as yet undefined nature of the receptor site—whether it is hydrophilic or lypophilic.

As a part of our on-going studies of neurotransmitters and related biomolecules[5a-i] we have investigated the shape of phenylethylamine by measuring and analyzing the millimeter-wave spectrum of phenylethylamine and its dideuteroisotopomer, deducing its shape from the derived values of the spectroscopic parameters of the molecule.

Previous Work

The low resolution electronic spectrum of phenylethylamine has been studied in the gas phase by Martinez *et al.*[6] In attempts to analyze the spectrum, an implicit assumption was made that there are spectral features that do not vary over a homologous series of molecules. Arguing by analogy with the systems of *n*-propylbenzene and tyramine, it was deduced that four peaks in the spectrum were attributable to two *gauche* conformers (τ_2 = 60°, see Figure 1) and two *trans* conformers (τ_2 = 180°), with the peaks for the *gauche* conformers being of greater intensity. However they did not achieve rotational resolution of their vibronic bands or present any other quantitative evidence that would help to provide positive structural identifications of the conformers, and so the identifications must be regarded as tentative.

The crystal structure analysis of the phenylethylamine hydrochloride showed that the ethylamine portion of the

[⊗] Abstract published in *Advance ACS Abstracts*, July 15, 1995.

(1) (a) Toufexis, A.; Bloch, H.; Donelly, S. B. *Time Magazine*; Melbourne, Australia, 15 February **1993**; 49−51. (b) *Elle*, May **1993**; 38−40.

(2) Borison, R. L.; Lemus, F.; Reyes, M.; Havdala, H. S.; Diamond, B. I. *Res. Comm. Psych. Psychiat. Behav.* **1977**, *2*, 193−201.

(3) Potkin, S. G.; Karoum, F.; Chuang, L. W.; Cannon-Spoor, H. E.; Phillips, I.; Wyatt, R. J. *Science* **1979**, *206*, 470−471.

(4) Paulos, M. A.; Tessel, R. E. *Science* **1982**, *215*, 1127−1129.

(5) (a) Uracil: Brown, R. D.; Godfrey, P. D.; McNaughton. D.; Pierlot, A. *J. Am. Chem. Soc.* **1988**, *110*, 2329−2330. (b) Adenine: Brown, R. D.; Godfrey, P. D.; McNaughton, D.; Pierlot, A. *Chem. Phys. Lett.* **1989**, *156*, 61−63. (c) Cytosine: Brown, R. D.; Godfrey, P. D.; McNaughton, D.; Pierlot, A. *J. Am. Chem. Soc.* **1989**, *111*, 2308−2310. (d) Thymine: Brown, R. D.; Godfrey, P. D.; McNaughton, D.; Pierlot, A. *J. Chem. Soc., Chem. Commun.* **1989**. 37−38. (e) Nicotinamide: Vogelsanger, B.; Brown, R. D.; Godfrey, P. D.; Pierlot, A. *J. Mol. Spectrosc.* **1991**, *145*, 1−11. (f) Histamine: Vogelsanger, B.; Godfrey, P. D.; Brown, R. D. *J. Am. Chem. Soc.* **1991**, *113*, 7864−7869. (g) 2-Pyridinone/2-hydroxypyridine: Hatherley, L. D.; Brown, R. D.; Godfrey, P. D.; Pierlot, A.; Caminati, W.; Damiani, D.; Favero, L. B.; Melandri, S. *J. Phys. Chem.* **1993**, *97*, 46−51. (h) Alanine: Godfrey, P. D.; Firth, S.; Hatherley, L. D.; Brown, R. D.; Pierlot, A. *J. Am. Chem. Soc.* **1993**, *115*, 9687−9691. (i) Glycine: Godfrey, P. D.; Brown, R. D. *J. Am. Chem. Soc.* **1995**, *117*, 2019−2023.

(6) Martinez III, S. J., III; Alfano, J. C.; Levy, D. H. *J. Mol. Spectrosc.* **1993**, *158*, 82−92.

0002-7863/95/1517-8204$09.00/0

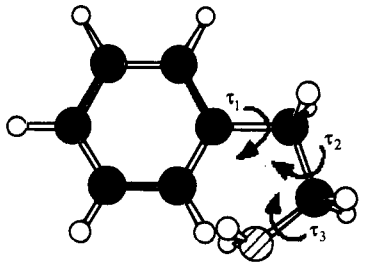

Figure 1. Reference conformation ($\tau_1 = \tau_2 = \tau_3 = 0°$) and definition of torsional angles for phenylethylamine conformers, where τ_3 is the dihedral angle between the bisector of the HNH angle and the C−C bond of the ethylamine group.

molecule is extended *(trans)* in the crystal.[7] However, this structural information concerns the phenylethylammonium cation. The network of hydrogen bonds and perhaps other lattice effects influence the structure observed.

Results from semiempirical calculations exploring the phenylethylamine potential energy surface indicate the folded *(gauche)* conformer is the preferred form.[8] The same workers also carried out single point calculations using *ab initio* methods and found that at the HF/STO-3G level the extended form was predicted to be more stable. Given the modest level of accuracy in the calculations performed thus far for phenylethylamine and the fact that there appears to be some ambiguity in the predicted shape, we have performed *ab initio* molecular orbital calculations using larger basis sets and including allowance for electron correlation at the MP2 level for all the possible structures as part of this work. The results play an important part in our study of the most stable conformers of phenylethylamine because we rely on them to indicate the most stable of the conformers (an uncertainty of a few kJ mol^{-1} being accepted) as well as defining the geometries of the conformers within narrow error bars (say within 1% for predicted rotational constants).

Experimental Section

The free-jet expansion, Stark-modulated spectrometer used in the present study has previously been described.[9] Liquid samples of phenylethylamine, obtained from Sigma Chemicals, were vaporized at 90 °C in a stream of argon at about 30 kPa and further heated to 120 °C before expansion through the jet. Broad band line-search scanning covered the entire range of the spectrometer, 48−72 GHz. Precise line frequencies were obtained from narrow band computer-averaged repetitive scans. Tables of measured frequencies are available as supporting information.

Monodeuterated phenylethylamine was prepared by stirring phenylethylamine with D_2O:H_2O = 1:1 under refluxing conditions for 3 h and then removing the water by rotary evaporation, leaving a mixture of d_0-, d_1-, and d_2-phenylethylamine. Both possible monosubstitutions on the amino nitrogen were obtained in sufficient quantities for their spectra to be observed and assigned. A sample of d_2-phenylethylamine also was obtained by using D_2O instead of D_2O/H_2O.

***Ab Initio* Calculations.** *Ab initio* calculations were performed using the GAUSSIAN 90 and 92 packages[10] at the RHF/4-21G, RHF/6-31G-(d,p), and MP2/6-31G(d,p) levels of approximation. Initially the phenyl ring was constrained to be planar. Such an approximation is widely accepted as making only very small changes in predicted spectroscopic constants, too small to influence the process of identification of conformers. To confirm this, we performed both unconstrained and planar-phenyl constrained optimizations using a small basis set (STO-3G), finding that rotational constants differed by only 2−4 parts per 1000, at least an order of magnitude smaller than would start to influence our conformational deliberations. Subsequent full optimizations with a 6-31G(d,p) basis and also at the MP2/6-31G(d,p) level confirmed that constrained planarity of the phenyl ring produced only very slight change in predicted rotational constants and dipole moment components.

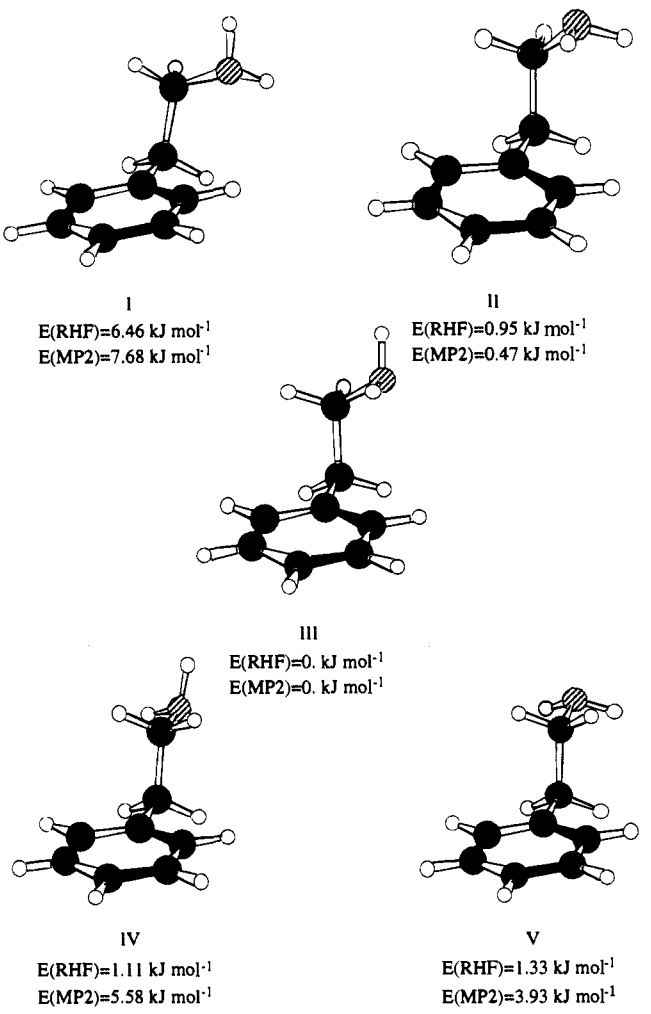

Figure 2. The five conformers found on the MP2 and RHF/6-31G** potential energy surfaces of phenylethylamine (RHF and MP2 relative energies given).

In the initial searching for conformers, i.e., domains within the potential energy hypersurface in which a local energy minimum occurs, energies were calculated, at the HF/4-21G level of theory, while the ethylamino torsional parameters τ_1, τ_2, and τ_3 (see Figure 1) were varied one at a time. Five domains were found: three *gauche* conformers differing in the orientation of the amino group (τ_3) and two with the nitrogen atom *trans* to the phenyl ring (Figure 2). All the conformers have τ_1 at 90° except conformer **I**, which has a τ_1 value of 124°. Their defining dihedral angles are given in Table 1. The most stable conformer at the HF/4-21G level of theory is the *gauche* conformer **II**, followed by **III**.

Five conformers were subsequently located on the HF/6-31G(d,p) and then the MP2/6-31G(d,p) potential energy surface of phenylethylamine, and these structures are shown in Figure 2. The optimized geometric parameters for the ethylamino group are listed in Table 1. A complete set of optimized structures is available as supporting information, and their derived spectroscopic parameters are listed in Table 2.

(7) Tsoucaris, P. G. *Acta Crystallogr.* **1961**, *14*, 909−914.
(8) Martin, M.; Carbo, R.; Petrongolo, C.; Tomasi, J. *J. Am. Chem. Soc.* **1975**, *97*, 1338−1347.
(9) Brown, R. D.; Crofts, J. G.; Godfrey, P. D.; McNaughton, D.; Pierlot, A. P. *J. Mol. Struct.* **1988**, *190*, 185−193.
(10) (a) Frisch, M. J.; Head-Gordon, M.; Trucks, G. W.; Foresman, J. B.; Schlegel, H. B.; Raghavachari, K.; Robb, M.; Binkley, J. S.; Gonzalez, C.; Defrees, D. J.; Fox, D. J.; Whiteside, R. A.; Seeger, R.; Melius, C. F.; Baker, J.; Martin, R. L.; Kahn, L. R.; Stewart, J. J. P.; Topial, S.; Pople, J. A. *Gaussian 90*, Revision I, Gaussian, Inc.; Pittsburgh PA, 1990. (b) Frisch, M. J.; Trucks, G. W.; Schlegel, H. B.; Gill, P. M. W.; Johnson, B. G.; Wong, M. W.; Foresman, J. B.; Robb, M. A.; Head-Gordon, M.; Replogle, E. S.; Gomperts, R.; Andres, J. L.; Raghavachari, K.; Binkley, J. S.; Gonzalez, C.; Martin, R. L.; Fox, D. J.; Defrees, D. J.; Baker, J.; Stewart, J. J. P.; Pople, J. A. *Gaussian 92/DFT, Revision G.3*; Gaussian, Inc.: Pittsburgh, PA, 1993.

Table 1. Optimized Geometric Parameters Obtained from 4-21G Basis Calculations for the Ethylamino Group for Phenylethylamine Conformers

	PEA I	PEA II	PEA III	PEA IV	PEA V
τ_1/deg	124.6	85.6	88.2	89.8	90.0
τ_2/deg	76.8	61.1	63.8	178.7	180.0
τ_3/deg	133.9	0.1	−132.1	132.8	0.0
E_{rel}/kJ mol^{-1}	3.53	0.0	0.24	1.99	0.90

Table 2. Molecular Parameters Predicted from *Ab Initio* Molecular Orbital Calculations [MP2/6-31G(d,p)][a]

	PEA I	PEA II	PEA III	PEA IV	PEA V
τ_1/deg	98.5	81.5	84.5	88.5	88.1
τ_2/deg	68.6	60.4	62.1	177.7	180.0
τ_3/deg	131.8	1.7	−125.1	125.5	0.0
E_{rel}/kJ mol^{-1}	7.68	0.47	0.0	5.58	3.93
A/MHz	3441.0	3278.4	3314.7	4378.6	4340.9
B/MHz	1071.9	1087.9	1101.8	861.8	859.6
C/MHz	905.3	963.3	964.7	771.1	769.2
$(B + C)$/MHz	1977.2	2051.2	2066.5	1632.9	1628.8
P_c/uÅ^2	30.1	47.0	43.6	23.2	23.7
μ_a/D	1.8	−0.9	−0.1	−0.1	−0.4
μ_b/D	−0.3	0.0	−0.7	1.1	−0.0
μ_c/D	−0.1	1.2	−1.1	−0.9	1.3
μ_{tot}/D	1.9	1.5	1.3	1.4	1.4
$\|a\|(H_{19})$/pm	321	160	314	396	397
$\|b\|(H_{19})$/pm	130	110	103	81	80
$\|c\|(H_{19})$/pm	25	124	152	26	24
$\|a\|(H_{20})$/pm	318	281	156		397
$\|b\|\|(H_{20})$/pm	114	157	112		80
$\|c\|(H_{20})$/pm	138	27	119	107	24
χ_{aa}/MHz	−2.5	−0.6	1.3	1.9	0.8
χ_{bb}/MHz	0.9	2.0	−0.1	−1.6	1.5

[a] For the amino-hydrogen numbering scheme see conformer **II** of Figure 2 in which the amino-hydrogen depicted as closer to the viewer is defined to be H_{19}. In the remaining conformers depicted, the amino-hydrogens H_{19} and H_{20} are related to conformer **II** by rotation about the C−N bond without N-inversion.

Relative Stabilities of the Conformers. The calculated relative stabilities of the conformers vary somewhat with the level of theory used (see Table 3). At the highest level used, phenylethylamine **III** is predicted to be the most stable conformer, followed by **II** and then **V**, the energy difference between **III** and **II** being small (39 cm^{-1}) while **V**, **IV**, and **I** are substantially higher in energy. At the RHF/6-31G-(d,p) level the differences in energy of **III** and **II** is greater, and **IV** and **V** are close in energy to **II**. At the 4-21G level the relative stabilities of **II** and **III** are reversed, and the energy separations of the other three less stable conformers are not as great as in the MP2 level calculations. Such variations in predicted relative energies of conformers when different levels of *ab initio* theory are used have been noted from time to time (see, e.g., 5f) and serve as a warning that although *ab initio* calculations are important in providing general indications of relative energies of conformers one must bear in mind that even MP2/6-31G(d,p) calculations cannot be relied upon to better than perhaps 100 cm^{-1} or so.

On the basis of the MP2/6-31G(d,p) calculations, differences in energies are such that in the vapor at 120 °C only **III** and **II** are expected to be present in high enough mole fraction to be detected in our jet spectrometer.

Some aspects of the relative stabilities of conformers can be accounted for by the fact that in conformers **II** and **III**, unlike the others, there is an amino hydrogen atom located over the phenyl ring. This interaction probably has a stabilizing influence through the formation of a weak hydrogen bond with the aromatic π-cloud acting as the electron donor and the amino hydrogens as electron acceptors. A stabilizing effect of this kind of interaction has been noted before in the case of histamine.[5f] An analogous bonding interaction between ammonia and benzene has also been reported more recently.[11] The distance of the nitrogen atom to the benzene plane was 359.0(5) pm. Using a typical N−H bond length of 108 pm, the distance of a hydrogen atom from the ring follows to be approximately 251 pm. The tilt angle between the C_3 symmetry axis of the ammonia and the benzene C_6 axis was found to be 59(5)°. This corresponds to a structure where one of the ammonia protons is pointing toward the center of the benzene ring.

Table 3. Relative Energies (cm^{-1}) of Conformers at Different Levels of *ab Initio* Theory

conformer	RHF/4-21G	RHF/6-31G(d,p)	MP2/6-31G(d,p)
I	301.4	539.8	641.7
II	0	79.4	38.8
III	30.6	0	0
IV	167.7	93.2	466.6
V	70.5	111.0	328.1

Table 4. Distances from the Amino Hydrogen to Their Nearest Ring Carbon Atoms, C_1 and C_6 for the MP2/6-31G(d,p) Structures

	phenylethylamine **II**	phenylethylamine **III**
$r(C_1, H)$/pm	269	264
$r(C_6, H)$/pm	278	269

For the *gauche* conformers **II** and **III**, which have an amino hydrogen located above the aromatic ring, Table 3 gives the distances from the amino hydrogen to their nearest ring carbon atoms, C_1 and C_6, for the MP2/6-31G(d,p) structures. C_1 is the ring carbon at which the ethylamine side chain is attached, C_6 being adjacent to C_1. From these one could conclude that phenylethylamine **III** is more stable than **II** because these distances are, on the whole, less for it than **II**. For a strongly hydrogen-bonded complex such as OCO···HF the O−H bond length is 191 pm.[12] The distances involved in phenylethylamine are much greater, which implies that these interactions should be significantly weaker. Given that the orientation of the amino group is the same for conformers **III** and **IV**, if the calculated energy difference (5.58 kJ mol^{-1}) is assumed, as an approximation, to represent the strength of this hydrogen bond, then the bond is substantially less than for OCO···HF [13.57 kJ mol^{-1} at the MP2/6-31G(d,p) level].

In association with the present studies, extensive *ab initio* calculations have been performed on the potential energy surfaces of related compounds such as β-aminoethylpyrrole and tryptamine from which it emerged that energetically appreciable interactions occur whenever one of the amino hydrogens is able to approach a carbon of an aromatic or heterocyclic ring from roughly above the ring plane to within about 250 pm or less.

Spectroscopic Parameters of the Conformers. From the data in Table 2, we see that the theoretical rotational constants of the *gauche* conformers, **I**, **II**, and **III**, are significantly different from those of the *trans* conformers **IV** and **V**. The *A* rotational constants are smaller, and the *B* and *C* values are greater. This contrast follows through in the planar moment P_c, for which conformers **II** and **III**, in particular, are set apart from the other conformers. Within the sets of *gauche* and *trans* conformers, the rotational constants are very similar, with the exception of conformer **I**, which has a larger *A* and smaller *C* value than **II** and **III**.

The total dipole moments of conformers **II**−**V** are nearly identical, although there is significant variation in the principal axis components. Both conformers **II** and **V** have low values for μ_b, whilst for **III** and **IV** μ_a is small. **III** and **IV** also have similar μ_b and μ_c values. If it is assumed that the intensity of a particular rotational transition is proportional to the square of the principal inertial axis dipole moment component connecting the two energy levels, it then follows for conformer **I** that there should not be any c-type transitions in its spectrum, similarly for **III** no a-type lines and for **V** no b-type lines.

Phenylethylamine **I** has a substantially greater dipole moment than the other conformers, having a large magnitude for μ_a. This can be rationalized by recognizing that the phenylethylamine dipole moment primarily originates from two centers: the amino group and benzene-alkyl linkage. Of the five conformers, **I** is the only conformer in which the group moments of the amino group and the benzyl group add constructively.

(11) Rodham, D. A.; Suzuki, S.; Suenram, R. D.; Lovas, F. J.; Dasgupta, S.; Goddard III, W. A.; Blake, G. A. *Nature* **1993**, *362*, 735−737.

(12) Baiocchi, F. A.; Dixon, T. A.; Joyner, C. H.; Klemperer, W. *J. Chem. Phys.* **1981**, *74*, 6544−6549.

Another discriminating feature between the five conformers is their substitution coordinates for the two amino hydrogens, all being notably different. This also is the case for the ^{14}N quadrupole coupling constants.

Results and Discussion

Approximately 70% of the lines observed were able to be assigned to two species. The predominant spectrum was assigned first and designated as belonging to species (x) and the less intense spectrum then to species (y). Recognizable patterns in the spectra of the two species meant that they were assigned without great difficulty. Within a given series, to which could be assigned a K_{-1} value, lines of consecutive J were separated by an approximate gap of 2 GHz ($\sim B + C$). For the (x) species, the $K_{-1} \leq 7$ lines showed quartet splitting. In the case of the (y) species, the low K_{-1} lines were split into doublets.

Rotational Constants and Planar Moments of Inertia. The experimentally derived rotational constants, which are shown in Table 5, indicate, by comparison with the *ab initio* predictions, that both species are *gauche* conformers because the predicted rotational constants of the *trans* structures are significantly greater. Conformer **I** can be eliminated because its A and C rotational constants are significantly different from those of both (x) and (y).

The planar moments of inertia $P_c = (I_1 + I_b - I_c)/2$ confirm that the observed species are most likely to be conformers **II** and **III**. Phenylethylamine (y) has the larger P_c value, and, of the theoretical conformers, this holds for conformer **II**. While this is an indication that species (y) might correspond to conformer **II** rather than conformer **III**, in isolation it is not sufficient to identify the species giving rise to the observed spectra.

Dipole Moments. For species (x), an unexpected Stark-pattern was observed for the transitions $12_{6,6}-11_{5,6}$ and $12_{6,7}-11_{5,7}$. On applications of an increasing electric field, the two composite lobes, with all their respective M components merged, initially begin approaching one another. At sufficiently high electric fields they coincide, and at higher fields the lobes continue to shift as a merged single lobe. A measured Stark effect line profile for these transitions is shown in Figure 3.

While not amenable to analysis by the conventional second-order perturbation theory treatment, this apparently bizarre Stark-shift behavior is adequately fitted with a full variational calculation that accommodates both degenerate and nondegenerate interactions. The $11_{5,6}$ and $11_{5,7}$ states are nearly degenerate and the $12_{6,6}$ and $12_{6,7}$ energy levels even more closely so. In the presence of an electric field, the two states in each degenerate pair interact by means of the μ_a dipole moment component. As a consequence, the $11_{5,6}$ state, for a particular M value, increases linearly in energy and the $11_{5,7}$ state decreases linearly in energy as the applied electric field is increased. There are, however, other nondegenerate energy levels that also are interacting with these states. The $10_{6,5}$ state, for example, lies only 2.7 GHz higher in energy and interacts with the $11_{5,6}$ state through μ_b to decrease the energy of the $11_{5,6}$ state through the quadratic Stark effect. A similar effect is observed for the $13_{6,7(8)}-12_{5,7(8)}$ transitions, which involve an analogous pattern of degeneracies. A representative value of $|M_J| = 1$ was adopted for the composite merged lobe in the fit of the dipole moment components to each of these transitions.

The measured Stark effect frequencies are available as supporting information. The electrode spacing was calibrated using the Stark effect of the $4_{1,3}-4_{1,4}$ transition of SO_2 (see footnote in supporting information). The measurements were used in a least-squares variational Stark effect computer program from which the best fit value of μ_a was determined to be 0.159(22) D and $(\mu_b^2 + \mu_c^2)^{1/2}$ 1.058(6) D. It was not possible to determine μ_b and μ_c separately because they were too highly correlated. Quantitative relative intensity measurements for b-type and c-type lines were precluded because at all practical modulating voltages there were slow moving Stark lobes under the zero-field lines which disturbed their measured intensities. The lines were, however, found to be of comparable intensity, and so it was possible to conclude that μ_b and μ_c are of similar magnitude for this conformer. For comparison, the MP2/6-31G** calculated dipole moment components are listed in Table 2. The calculated value of $(\mu_b^2 + \mu_c^2)^{1/2}$ is 1.3 D for both theoretical conformers **III** and **IV**. With their small μ_a values and similar magnitudes for μ_b and μ_c it is not clear from the predicted dipole moment components alone which of these two is the better match for species (x). However, phenylethylamine **IV** is a less likely candidate considering the poor agreement between its rotational constants and those of species x.

For the less abundant species (y), it was not possible to measure the dipole moment components via Stark shifts. There were no transitions for which the M components clustered together, as was found for (x). Relative intensities were employed to aid in identifying conformers. The spectrum was dominated by c-type lines. In cases where the b-type lines were predicted to be clear of overlap with the c-type transitions, in the $K_a = 6$ series, for example, no b-type lines were observed. This indicates that μ_b is very small relative to μ_c.

Table 5. Experimentally Derived Rotational Constants for Phenylethylamine

	phenylethylamine(x)	phenylethylamine(y)
A/MHz	3313.7472(32)	3287.7120(42)
B/MHz	1079.2824(22)	1066.3587(84)
C/MHz	959.2010(23)	957.6377(70)
D_J/kHz	0.2024(25)	0.2219(45)
D_{JK}/kHz	0.7974(96)	0.909(15)
D_K/kHz	0.442(24)	0.324(38)
P_c/uÅ^2	46.944	49.956
no. of lines in fit	58	48
RMS error in fit/kHz	39	48

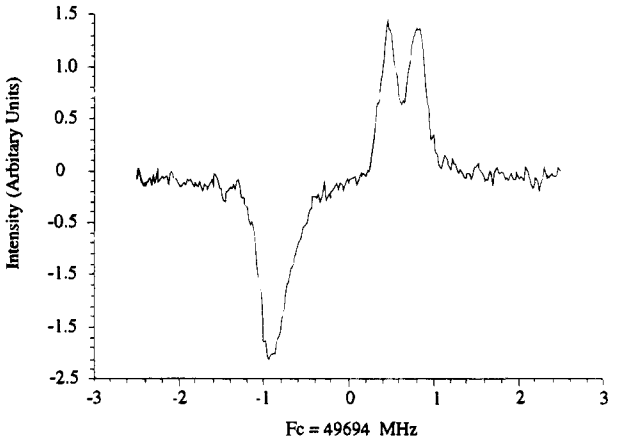

Figure 3. Stark pattern observed for the transitions $12_{6,6}-11_{5,6}$ and $12_{6,7}-11_{5,7}$.

Table 6. Experimentally Derived Rotational Constants for Phenylethylamine-Nd_2

	PEA(x)-Nd_2	PEA(y)-Nd2
A/MHz	3191.552(44)	3178.331(45)
B/MHz	1043.94(23)	1038.87(49)
C/MHz	932.43(19)	932.19(43)
D_{JK}/kHz	1.41(27)	1.47(28)
no. of lines in fit	26	21
RMS error in fit/kHz	484	402
P_c/uÅ^2	50.23	51.67

Table 7. Predicted Rotational Constants for All the Amino Hydrogen Isotopomers Shown in Comparison with the Constants Fitted to the Observed Spectra[a]

		gauche			*trans*			
		PEA I	PEA II	PEA III	PEA IV	PEA V	PEA(x)	PEA(y)
NH_2	*A*/MHz	3543.6	3394.9	3424.2	4528.1	4504.9	3313.7	3287.7
	B/MHz	1045.5	1048.4	1060.6	852.7	850.4	1079.3	1066.3
	C/MHz	887.9	938.5	936.8	763.1	760.5	959.2	957.7
	(*B* + *C*)/MHz	1933.4	1986.9	1997.4	1615.8	1610.9	2038.5	2024.0
ND_2	*A*/MHz	3435.1	3279.9	3301.1	4461.3	4448.2	3191.6	3178.3
	B/MHz	997.4	1019.2	1022.4	805.2	807.0	1043.9	1038.9
	C/MHz	851.8	913.1	909.1	725.1	724.4	932.4	932.2
	(*B* + *C*)/MHz	1849.1	1932.3	1931.5	1530.3	1531.4	1976.3	1971.1
	Δ*A*/MHz	108.5	115.0	123.1	66.8	56.7	122.1	109.4
	Δ*B*/MHz	48.1	29.2	38.2	47.5	43.4	35.4	27.4
	Δ*C*/MHz	36.1	25.4	27.7	38.0	36.1	26.8	25.5
ND	*A*/MHz	3503.7	3330.1	3359.2	4499.3	4477.3	3244.7	3227.2
	B/MHz	1022.3	1037.3	1031.8	830.43	827.90	1051.2	1056.5
	C/MHz	868.9	931.2	916.3	744.6	741.9	939.7	951.2
	(*B* + *C*)/MHz	1891.2	1968.5	1948.1	1575.0	1569.8	1990.9	2007.7
ND'	*A*/MHz	3471.6	3340.8	3360.8	4490.9	4477.3	3255.6	3235.0
	B/MHz	1019.3	1029.8	1050.3	825.7	827.9	1070.5	1047.6
	C/MHz	869.7	919.9	929.3	742.3	741.9	952.5	938.8
	(*B* + *C*)/MHz	1889.0	1949.7	1979.6	1568.0	1569.8	2023.0	1986.4

[a] The label ND refers to deuterium substitution at amino-hydrogen H_{19} and ND' to substitution at H_{20}. (See footnote Table 2.)

Some a-type lines were seen but their intensities were low in comparison to the c-type lines. This was because given the frequency region being studied, there were exclusively high-*J* a-type transitions which, at the low rotational temperatures of our studies, involved energy levels that were not heavily populated. Taking these facts together, the relative intensities support the identification of species (y) as being conformer **II** or **V**. However, (y) is less likely to be identified as phenylethylamine **V** considering the poor match between their rotational constants.

Using the theoretical dipole moment components of phenylethylamine **II**, for all appropriate transitions Stark patterns were predicted. Some exhibited modulatable but unresolvable Stark components resulting in one rather broad and featureless composite lobe. With the other modulatable transitions the *M* components were resolvable, but it was clear that the sensitivity of the spectrometer would be insufficient to detect the many weak *M* components into which these high *J* transitions (typical of the frequency region) were split by the Stark effect.

Since each spectrum was predominantly c-type, and reasonably assuming that μ_c for the two conformers is approximately the same, it appears that (x) is present in the gas phase in greater abundance since it has a more intense spectrum. We prefer not to offer a more quantitative estimate because of uncertainties in the values of dipole moment components and difficulties relating to overlapping lines and degree of modulation of lines.

Deuterated Isotopomers. Spectra for the dideutero isotopomers were detected, measured, and assigned. Frequency patterns, relative line intensities, and Stark effects were found to resemble those in the parent species spectra. The measured frequencies are available as supporting information, and the fitted spectral parameters are given in Table 7. The frequencies were simply measured from the broad band scan chart because the sole purpose was to distinguish them from the monodeutero spectra. The *ab initio*-predicted rotational constants for all the amino hydrogen isotopomers are shown in comparison with the constants fitted to the observed spectra in Table 7. The change in the rotational constants on dideuteration lends tentative support to the assignment of (x) to conformer **III** and (y) to conformer **II**.

Identification of the monodeuterated species with their corresponding spectra proceeded as for the dideutero isotopomers. The measured frequencies are available as supporting information, and the fitted spectral parameters are given in Table 8 for phenylethylamine(x)-d_1 and in Table 9 for phenylethylamine(y)-d_1. Using Kraitchman's equations, the principal axis substitution coordinates for each of the amino hydrogens were calculated from the changes in the principal moments of inertia upon deuteration. Presented in Table 10, they lend strong support to the match of conformer (x) to phenylethylamine **III** and (y) to **II**.

Table 8. Fitted Spectral Parameters for Phenylethylamine(x)-Nd_1

	PEA(x)-Nd_1	PEA(x)-Nd_1'
A/MHz	3244.7384(30)	3255.6185(60)
B/MHz	1051.182(17)	1070.479(21)
C/MHz	939.709(15)	952.508(18)
D_J/kHz	0.1978(53)	0.1980(83)
D_{JK}/kHz	0.770(24)	0.853(37)
D_K/kHz	0.472(37)	0.276(66)
P_c/uÅ^2	49.361	48.380
no. of lines in fit	41	41
RMS error in fit/kHz	25	36

Table 9. Fitted Spectral Parameters for Phenylethylamine(y)-Nd_1

	PEA(y)-Nd_1	PEA(y)-Nd_1'
A/MHz	3227.2382(39)	3235.0066(42)
B/MHz	1056.528(38)	1047.617(39)
C/MHz	951.196(33)	938.837(35)
D_J/kHz	0.2453(87)	0.239(10)
D_{JK}/kHz	0.770(24)	0.688(45)
D_K/kHz	0.213(60)	0.648(63)
P_c/uÅ^2	51.814	50.163
no. of lines in fit	35	34
RMS error in fit/kHz	34	38

The standard deviations calculated for the coordinates incorporated the contributions from both the variances and covariances of the rotational constants. For both of the monodeutero isotopomers of (y), the covariances between the *B* and *C* rotational constants were large. The consequent propagated variances in the coordinates, although larger than those for (x), were not substantial.

Quadrupole Hyperfine Splitting. It was possible to observe resolved ^{14}N quadrupole hyperfine patterns only for some very weak lines. These transitions usually involved changes of three in the K_{-1} pseudo quantum number. In Figure 4 the hyperfine patterns for the five theoretical conformers of phenylethylamine are presented for the $15_{3,12}-14_{0,14}$ transition. The predicted fully resolved unsymmetrical doublet patterns of the conformer pair

Table 10. Principal Axis Substitution Coordinates for the Amino Hydrogens

	MP2/6-31G(d,p)					experimental	
	PEA I	PEA II	PEA III	PEA IV	PEA V	PEA x	PEA y
$\|a\|(H_{19})$/pm	321	159	314	395	398	316.712(33)	159.29(11)
$\|b\|(H_{19})$/pm	130	109	103	85	81	90.75(49)	100.65(94)
$\|c\|(H_{19})$/pm	24	124	152	22	22	158.68(27)	137.62(68)
$\|a\|(H_{20})$/pm	318	281	156	424	398	154.97(10)	286.791(66)
$\|b\|(H_{20})$/pm	115	157	112	12	81	112.74(44)	153.93(70)
$\|c\|(H_{20})$/pm	137	28	119	106	21	121.51(40)	45.2(24)
dev(x)/pm[a]	90	88	13	135	126		
dev(y)/pm[a]	95	9	93	136	122		

[a] For each of the conformers PEA (**I**–**V**), the quantities dev(x) and dev(y) are the rms deviations of the six theoretical *ab initio* nuclear coordinates listed in the column above, from the corresponding tabulated experimental values at right, for the observed species PEA x and PEA y, respectively.

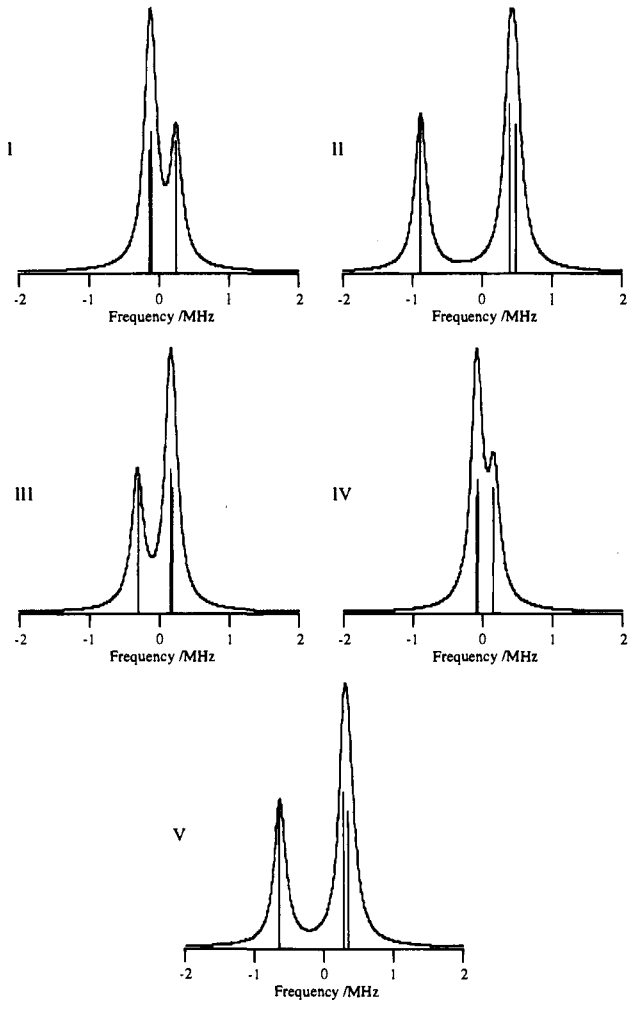

Figure 4. Predicted [MP2/6-31G(d,p)] ^{14}N quadrupole hyperfine patterns for the $15_{3,12}-14_{0,14}$ transition for phenylethylamine conformers **I**–**V**.

II and **V** are virtually indistinguishable as are the merged doublets of the pair **I** and **IV**. Conformer **III** stands out as the only merged doublet with the weaker component to lower frequency. The observed hyperfine patterns of species (x) and (y) are shown in Figure 5. For species (x) there is a shoulder to low frequency of the more intense peak, and this is consistent with the predicted pattern of conformer **III**. The observed resolved unsymmetrical doublet hyperfine pattern of species (y) is consistent with those predicted for conformers **II** and **V**. Given that both predicted hyperfine patterns are quite similar, it is not possible to identify species (y) with one particular conformer on hyperfine evidence alone. However, on consideration of the

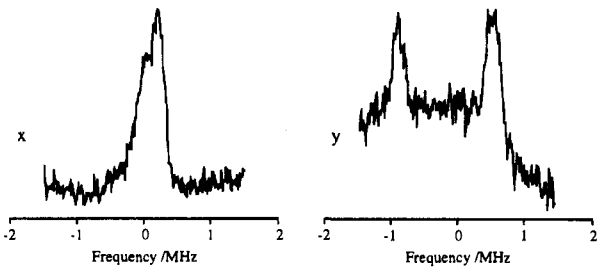

Figure 5. Observed ^{14}N quadrupole hyperfine patterns for the transition $15_{3,12}-14_{0,14}$ phenylethylamine (x) and (y). The integration time was 120 min for (x) and 540 min for (y). The plot center frequencies are 59 243.0 MHz for (x) and 57 644.5 MHz for (y). Theoretical rotational frequencies calculated using the least-squares fit rotational and centrifugal distortion constants given in Table 4 are 50 243.2 MHz for (x) and 57 664.3 MHz for (y).

all the preceding results, (y) can be identified confidently as phenylethylamine **II**.

Inversion Splitting. For many molecules containing an amino group, such as ammonia, aniline, and methylamine, their spectra exhibit splitting due to inversion motions. In the case of the simpler homologue of phenylethylamine, ethylamine, inversion splitting was observed for the *gauche* conformer but not the *trans*.[13] In contrast, there were not signs of such splitting in either of the spectra for the two phenylethylamine species, lending support to the idea that an amino hydrogen is attracted to the aromatic ring through a hydrogen bond-like interaction in both conformers, resulting in inhibition of the inversion vibration.

Unassigned Lines. An attempt was made to assign the remaining lines but this was unsuccessful. They are substantially weaker than the assigned lines. Patterns, in lines separated by $(B + C)$ equal to approximately 1600 MHz, would have been observed for any *trans* conformer of phenylethylamine. The tabulated lines show no evidence for *trans* conformers in this work. This contrasts with the conclusions of Levy *et al.*[6] In their low resolution spectroscopic analysis of phenylethylamine, they claimed there were two *trans* as well as two *gauche* conformers. Their only evidence for identification of the conformers was an assumption of similarity to vibronic bands for some related molecules, and so their conclusions must be considered very tentative. However, since helium, which Ruoff et al.[14b] found to produce no conformational relaxation, was used by Levy et al. and we used argon, which is much more effective in producing relaxation, it is possible that Levy et al. observed conformers **IV** and **V**, while in our jet these two relaxed to **III** and/or **II**.

Conformer Relaxation in Jet. In jet spectroscopy two factors can affect conformer populations. Firstly conformers that are not thermally accessible in the vapor before jet expansion will not be present in detectable amounts after expansion. Secondly, those conformers that are thermally accessible at the pre-expansion temperature may relax to lower-energy conformers during the expansion if the barrier heights are sufficiently low.

Studies of conditions in supersonic expanding jets of noble gases[14] indicate that in our argon jet the relaxation of conformer **II** to **III** would be complete if the barrier to isomerization is low enough (say less than 500 cm^{-1} [6 kJ mol^{-1}]). Under these conditions **II** would be present in relative abundance of 0.4% compared with **III**, based on a jet rotational temperature of 10 K and MP2/6-31G(d,p) relative energies. From a comparison

(13) Fischer, E.; Botskor, I. *J. Mol. Spectrosc.* **1982**, *91*, 116–127.
(14) (a) Felder, P.; Günthard, Hs. H. *Chem. Physics* **1982**, *71*, 9–25. (b) Ruoff, R. S.; Klots, T. D.; Emilsson, T.; Gutowsky, H. S. *J. Chem. Phys.* **1990**, *93*, 3142–3150. (c) Godfrey, P. D.; Brown, R. D.; Rogers, F. M. Submitted for publication.

of line intensities (and assuming that μ_c is approximately the same for both conformers), **III** is observed to be present in the expanded jet stream in greater abundance than **II** by about a factor of three. It follows that relaxation of **II** to **III** does not occur and that the barrier to the interconversion is greater than 500 cm^{-1}.

We investigated the barrier height with a series of MP2/6-31G(d,p) calculations in which the dihedral angle τ_3 was stepped through values that corresponded to the **II** → **III** conversion, all other geometric parameters being optimized at each point. This gave an estimate of the barrier of 1140 cm^{-1}. We similarly estimated barriers of 1120 cm^{-1} for **IV** → **V** and 1530 cm^{-1} for **IV** → **III** although these data are of academic interest for the present jet spectroscopy study. In contrast, the barrier to relaxation for **I** → **III** was estimated to be only 270 cm^{-1}, low enough for relaxation to occur in the jet, but again the mole fraction of **I** is estimated to be too low at 120 °C for this situation to have relevance to our present observations.

Summary and Conclusions

The rotational spectra of two species of phenylethylamine, (x) and (y), have been assigned and identified as belonging to the two *gauche* conformers **III** and **II**, respectively (see Figure 2). The amino hydrogen principal axis substitution coordinates and the ^{14}N quadrupole hyperfine pattern clearly indicate that (x) is conformer **III**. The measured dipole moment components also confirm this. Given the evidence presented from the deuterated data and the semiquantitative estimate of the dipole moment components from intensities, species (y) is identified as phenylethylamine **II**.

The observation of these two conformers is in accordance with the relative energy predictions from *ab initio* molecular orbital calculations. On the basis of the energy difference for **III** and **II**, 0.47 kJ mol^{-1}, if the equilibrium was frozen at the jet temperature of 120 °C we would expect the abundance ratio to be 1:0.87. This would be altered if there were a difference in zero-point energies, but the two conformers differ so little in shape and general physical nature that we expect these energies to differ insignificantly.

The calculated relative energies of other conformers indicate that they would not be present in sufficient quantities in our jet spectrometer for them to be detected.

Acknowledgment. This work was supported by grants from the Australian Research Council.

Supporting Information Available: A listing containing the complete *ab initio* optimized geometries for each theoretical conformer and all the measured and assigned microwave transition frequencies used to derive the rotational constants reported in this work as well as the Stark effect measurements used in fitting the dipole moment of conformer (x) (18 pages). This material is contained in many libraries on microfiche, immediately follows this article in the microfilm version of the journal, can be ordered from the ACS, and can be downloaded from the Internet; see any current masthead page for ordering information and Internet access instructions.

JA951106A